

A comparative study of dosimetric parameters of 3D-printed non-coplanar template-assisted CT-guided iodine-125 seed implantation brachytherapy in patients with inguinal lymph node metastatic carcinomas

Yanhao Liu, MD*, Zongyan Shen, MD*, Ang Qu, MD, Ping Jiang, MD, Yuliang Jiang, MM, Junjie Wang, MD, PhD

*Yanhao Liu and Zongyan Shen are joint first authors.

Department of Radiation Oncology, Peking University Third Hospital, Beijing, China

Abstract

Purpose: To compare the pre-plan and post-plan dosimetric parameter differences of 3D-printed non-coplanar templates (3D-PNCT)-assisted computed tomography (CT)-guided iodine-125 (¹²⁵I) radioactive seed implantation brachytherapy (RISI) in patients with inguinal lymph node metastasis (ILNM).

Material and methods: This was a retrospective study of 15 patients with ILNM carcinomas treated with 3D-PNCT-assisted CT-guided RISI between May, 2015 and April, 2018. All patients underwent prior external beam radiotherapy (EBRT) or surgery. Dosimetric parameters included D₉₀, D₁₀₀ (dose delivered to 90% and 100% of the volume, respectively), V₁₀₀, V₁₅₀, V₂₀₀ (percentage of target volume receiving 100%, 150%, and 200% of the prescribed dose, respectively). Quality parameters included conformal index (CI), external index (EI), and homogeneity index (HI). Paired *t*-test and Bland-Altman analysis were applied to compared pre-plan and post-plan parameters.

Results: The median gross tumor volume (GTV) in the pre-plan was 8.7 ml (range, 0.8-185.1 ml). There were statistically significant differences in V₁₀₀, V₁₅₀, CI, and EI (*p* < 0.05). Bland-Altman analysis indicated that accidental error of RISI was small. In 1 of the 15 cases, D₉₀ and D₁₀₀ exceeded the prescribed therapeutic accuracy. In 1 of the 15 cases, V₁₅₀, EI, and GTV were outside the specified accuracy range (95% confidence interval).

Conclusions: 3D-PNCT-assisted CT-guided RISI is a safe, accurate, and feasible choice in ILNM treatment. The procedure of RISI has significantly improved. The pre-plan can be accurately executed by 3D-PNCT-assisted CT-guided RISI.

J Contemp Brachytherapy 2022; 14, 5: 452-461

DOI: <https://doi.org/10.5114/jcb.2022.121564>

Key words: interstitial permanent brachytherapy, inguinal lymph node metastasis, 3D printing non-coplanar template, ¹²⁵I radioactive seed implantation.

Purpose

Inguinal lymph nodes (ILN) are divided into superficial and deep groups. The superficial ILN lie immediately below the inguinal ligament and are divided into three groups: superomedial, superolateral, and inferior. The deep ILN lie medial to the femoral vein under the cribriform fascia, and drain superiorly to the external iliac, pelvic, and para-aortic lymph nodes in turn. Inguinal lymph node metastatic (ILNM) carcinomas occur commonly in patients with colorectal cancer, penile cancer, gynecolog-

ical tumors, and other pelvic malignant neoplasms [1-3]. Surgical resection or external beam radiotherapy (EBRT) is the first-line treatment in patients with ILNM carcinomas, dependent on the number or the extent of lesions. For patients with recurrent disease, the prognosis is very poor, and alternatives for salvage treatment are limited. Repeated surgical dissection is challenged by high-risk of lymphedema of the limbs. Although re-irradiation is an option, it is difficult to deliver high doses sufficiently to lesions previously treated with EBRT due to concerns on the effects of radiotherapy toxicity, including fibrosis,

Address for correspondence: Junjie Wang, MD, PhD, Department of Radiation Oncology, Peking University Third Hospital, No. 49 North Huayuan Road, Beijing 100191, China, phone: +86-18910592802, e-mail: junjiewang_edu@sina.cn

Received: 11.06.2022

Accepted: 11.10.2022

Published: 30.11.2022

lymphedema, and function disorder of the lower limbs. Meanwhile, chemotherapy is mostly used as a palliative treatment option [1-6].

Iodine-125 (^{125}I) radioactive seed implantation (RISI) plays an important role in the treatment of prostate cancer, either as monotherapy or in combination with EBRT [7]. Indeed, RISI can be applied in various tumors sites as the primary treatment or to boost the effects of EBRT. RISI has been shown to be precise and accurate under image guidance, and the needle puncture procedure is minimally invasive compared with surgery or EBRT. Computed tomography (CT)-guided RISI has been successfully applied in head and neck, thoracic, abdomen, pelvic, and retro-peritoneal and spinal malignancies [8-11]. Indications for RISI are expanding rapidly, especially for recurrent carcinoma following EBRT.

In 2015, the 3D-printing template technique has been integrated into the treatment of body carcinomas in our institution. Thereafter, the safety, accuracy, and feasibility of 3D-printed non-coplanar templates (3D-PNCT) application in various tumors and locations was explored [12-14]. In this retrospective study, the pre-plan and post-plan dosimetric parameters of 3D-PNCT-assisted CT-guided RISI in ILNM patients were analyzed.

Material and methods

Indication, patient selection, and preparation for RISI

In our retrospective study, 15 patients with ILNM carcinomas treated with RISI between May, 2015 and April, 2018 were involved. Inclusion criteria were as follows: 1) Karnofsky performance status (KPS) score ≥ 60 ; 2) Expected survival ≥ 3 months; 3) Pathological or radiological diagnosis of ILNM carcinoma; 4) Ability to design suitable needle paths; 5) No systemic metastasis or with stable oligo-metastasis (≤ 3 lesions); 6) Non-surgical candidate or unresectable tumor; and 7) Refusal of EBRT. Exclusion criteria were as follows: 1) Severe organ dysfunction; 2) Coagulation dysfunction; 3) Recent anticoagulant therapy and infection; 4) Mental illness; and 5) Extensive skin necrosis, fistula, and ruptured skin. All participants provided written informed consent. The protocol of the study was approved by the Ethics Committee of Peking University Third Hospital (approval No.: IRB00006761-M2019118).

The selected patients underwent CT simulation immobilized with a vacuum pad in a supine position. CT (Brilliance, Philips Inc., The Netherlands) scan with a contrast was performed, with a slice thickness of 5 mm. Positioning of X-axis and Y-axis lines, and alignment reference laser line were marked on the skin surface of patient. CT images were transferred to brachytherapy treatment planning system (BT-TPS, KLSIRPS-3D, Beijing Tianhang Kelin Technology Development Inc., China) for pre-planning. Gross tumor volume (GTV) was defined as palpable or visible extent, and location of malignancies diagnosed as ILNM pathologically or through clinical imaging. Skin, intestine, and femoral head adjacent to lesions were defined as organs at risk (OARs). Both targets and OARs were

delineated in BT-TPS. Clinical tumor volume (CTV) was a 3 mm expansion of GTV in three dimensions (3D). Needles pathways (direction, depth, and distribution) in the target were designed in BT-TPS (Figure 1B-D), and if possible, needles were arranged in parallel way. Meanwhile, blood vessels, bony structures, and nerves were avoided or kept away from needle channels, with a safety distance of 0.5-1 cm. Spatial distribution of ^{125}I seeds was simulated, and dose distribution in the target and OARs was calculated. Dose received by 90% of GTV (GTV D_{90}) was intended to be as close as possible to prescription dose (PD), whereas dose received by OARs was kept as low as possible (Figure 1E). Prescription dose was 120 Gy, and D_{max} (maximum dose) of the skin was kept below 50 Gy. In general, D_{max} of the intestine and femoral head were so low that there was no need for relevant limiting criteria. This enabled target conformality to meet the pre-plan requirement, while limiting doses to surrounding tissues.

3D-PNCT design and production

Data in BT-TPS were imported to Magics 19.01 (Materialise, Belgium) for digital modeling of the individualized 3D-PNCT. Information about the needle path direction was added to the model. 3D-PNCT was printed out by a 3D light-cured rapid-forming printer (RS6000, Shanghai Liantaiv3D Technology Company Inc., China). 3D-PNCT included surface characteristics of the patient, needle holes, X-axis and Y-axis coordinate registered marks, and the number of simulated needle paths. Three needle holes were used to fix the alignment of 3D-PNCT onto patients.

Workflow of RISI

The RISI workflow included the following 8 steps: 1) Patient was set-up on CT-simulator and immobilized with a vacuum pad. Local anesthesia was carried out. 3D-PNCT was aligned to the patient body surface by X-axis and Y-axis positioning reference lines (Figure 1A). Three stable needles were inserted into the patient's body at a depth of 2-3 cm to fix 3D-PNCT; 2) CT scan was performed to verify the direction and depth of stable needles to ensure that 3D-PNCT was positioned accurately; 3) If the position of the stable needles between the actual image and pre-plan image was mismatched, the needles and template were fine-tuned in real-time according to offset direction and distance, then returned to step 2; 4) Seed needles were all inserted into the targets (Figure 1H); 5) CT scan was performed to confirm the direction and depth of the needles (Figure 1F); 6) If the deviation was more than 3 mm, fine adjustments would be made according to the offset direction and distance, then returned to step 5; 7) ^{125}I seed (^{125}I seed: 6711-99, length: 4.5 mm, diameter: 0.8 mm, half-life: 59.4 days; Beijing Atom High Tech Pharmaceutical Company Inc., China) implantation was delivered with an applicator (Mick200-TPV applicator, Mick Radio-Nuclear Inc., USA); and 8) CT scan was performed again to observe the actual distribution of ^{125}I seeds in the targets. CT images were transferred into BT-TPS for post-plan dose evaluation (Figure 1G). Patients were discharged 1-2 days after RISI. All procedures

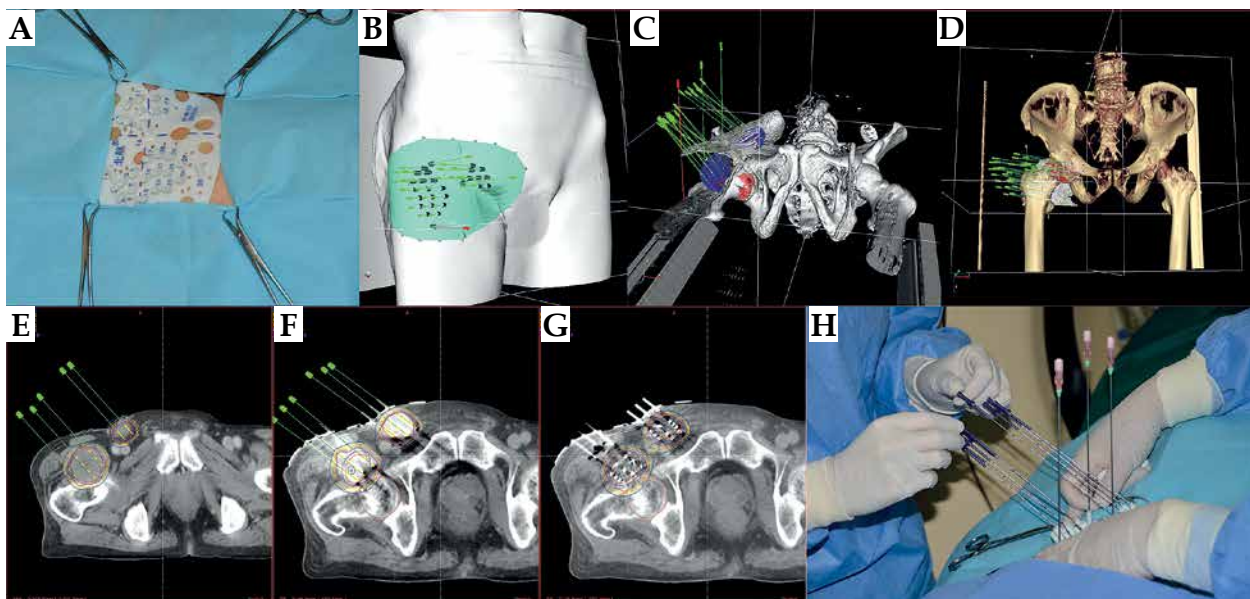


Fig. 1. Photos and treatment plans of ^{125}I radioactive seed implantation brachytherapy (RISI). **A)** 3D-printed non-coplanar templates (3D-PNCT) aligned to the patient. **B-D)** Visualization of pre-plan. **E)** Pre-plan. **F)** Intra-operative plan. **G)** Post-plan. **H)** Implementation of RISI

followed the International Commission on Radiological Protection recommendations [15].

During the course of treatment, at least four CT scans were performed for each patient: CT-simulation, after stable needle insertion, after seed needle insertion, and after RISI. If fine adjustments were made, more CT scans would be performed. The median number of CT scans of each patient was 4 (range, 4-6 scans).

The following might occur during operation: 1) Tumor displacement or deformation caused by puncture; 2) Needle tip position deviation > 3 mm; and 3) Changes in seeds spacing and direction after needle extraction. In these situations, the depth of needles or seeds distribution were adjusted to meet dose requirements.

Post-plan evaluation of dosimetric parameters

The following data were defined and recorded: doses delivered to 90% (D_{90}) and 100% (D_{100}) of GTV; percentage of GTV receiving 100% (V_{100}), 150% (V_{150}), and 200% (V_{200}) of the PD; external index (EI), conformal index (CI), and homogeneity index (HI) of the targeted area.

The conformity of dose distribution was evaluated by CI. $CI = (VT_{ref}/VT) \times (VT_{ref}/V_{ref})$, where VT was the volume of GTV (ml), VT_{ref} was the volume of GTV, in which the dose exceeded the prescribed dose, and V_{ref} was the total volume, in which the dose exceeded the prescribed dose. The best CI was 1, which indicated that GTV was just covered by the prescribed dose, and the dose outside GTV was lower than the prescribed dose [16].

The volume exceeding PD outside GTV was described by EI. $EI = (V_{ref} - VT_{ref})/VT$. The greater the value of the EI, the greater the recommended dosage received outside GTV [16].

The uniformity of dose distribution was evaluated by HI. $HI = (VT_{ref} - VT_{1.5ref})/VT_{ref}$ where $VT_{1.5ref}$ was the

volume of GTV, in which the dose exceeded 1.5 times of the prescribed dose. The closer to 100% of HI, the more uniform the dose distribution of GTV [16].

Follow-up and examinations

Follow-up assessments were performed at 3, 6, 9, and 12 months after RISI, and then every 6 months after one year. The assessments involved regular outpatient visits and telephone interviews. Diagnostic imaging with CT scans or magnetic resonance imaging (MRI) examinations was used to evaluate tumor response for each post-operative visit.

Primary end-points included: (1) Dosimetric parameters, such as D_{90} , D_{100} , V_{100} , V_{150} , and V_{200} ; (2) Quality parameters, including CI, HI, and EI; (3) Perioperative complications of puncture-related procedures, such as bleeding, infection, fever, and impaired lower limb motor function; and (4) Acute and late radiation toxicity. Adverse events were evaluated according to criteria established by the Radiation Therapy Oncology Group (RTOG) and the European Organization for Research and Treatment of Cancer (EORTC) [17].

Second set of endpoints included local tumor response, local control (LC), overall survival (OS), progression-free survival (PFS), and pain relief. Criteria from the response evaluation criteria in solid tumors (RECIST) version 1.1 were applied to measure the local tumor response at one month after RISI. Subsequently, routine follow-ups were conducted to determine LC, OS, and PFS. Pain was assessed with numerical rating scale (NRS), which was categorized into five grades: 0 - no pain, 1-3 - mild pain, 4-6 - moderate pain, 7-9 - severe pain, and 10 - unbearable pain. The pain score at one month after treatment was compared with that before treatment.

Statistical analysis

Statistical analysis was performed using SPSS version 25.0 (IBM Corp., Armonk, NY, USA). Paired sample *t*-test was used to compare the means of pre-operative and post-operative dosimetric parameters. Kaplan-Meier survival analysis was applied to estimate LC, PFS, and OS. R-3.6.2 (Lucent Technologies Inc., New Jersey, USA) was used to build box-whisker plots to visualize the numerical value and distribution of parameters. Bland-Altman method was applied to analyze the accidental factors of pre-operative and post-operative dosimetric parameters with MedCalc version 15.2.2 software. *P*-value < 0.05 was considered statistically significant.

Results

A total of 15 patients with ILNM successfully received RISI between May, 2015 and April, 2018. The median follow-up time was 23 months (range, 3-48 months), and 6 patients were still alive at the end of the study. There were 6 males and 9 females, with a median age of 61 years (range, 28-77 years). Of the 15 patients, 10 had primary tumors of the genitourinary system, 3 of the digestive system, and 2 patients suffered from sarcomas. Additionally, 11 patients underwent prior EBRT and 11 underwent previous surgery; twelve patients suffered from pain before RISI (Table 1). The median seed apparent activity was 0.6 mCi (range, 0.50-0.78 mCi), the median number of needles was 9 (range, 4-36 needles), and the median seed number was 37 (range, 8-121 seeds) (Figure 2A). The numerical value and distribution of pre-plan and post-plan parameters are presented in Table 2 and Figure 2B-F.

There were no perioperative period complications, such as bleeding, infection, fever, neurological, limb function disorders, or seed migration. In eleven patients, pain was relieved or downgraded after RISI. In terms of grade 1 side effects, two patients suffered from skin injury, and one patient experienced urinary system reaction. No grade 2 or above toxicities were observed.

The result of paired sample *t*-tests are presented in Table 2. The differences of pre- and post-plan D_{90} , D_{100} , V_{200} , HI, and GTV were not statistically significant ($p > 0.05$), while the differences of pre- and post-plan V_{100} , V_{150} , CI, and EI were statistically significant ($p < 0.05$).

Using Bland-Altman analysis, the abscissa was the value of pre-plan dose parameter, the ordinate was the difference between the pre-plan and post-plan parameters, and the mean of difference was ± 1.96 time; standard deviation of the difference was 95% confidence interval (95% CI) for plotting the scatter plot (Figure 3). D_{90} (Figure 3A), D_{100} (Figure 3B), V_{150} (Figure 3D), EI (Figure 3G), and GTV (Figure 3I) were outside 95% CI in 6% (1/15) of patients. V_{100} (Figure 3C), V_{200} (Figure 3E), CI (Figure 3F), and HI (Figure 3H) were within the 95% CI.

Complete response (CR) was observed in 9/15 (60%) of the patients, partial response (PR) in 4/15 (27%), and stable disease (SD) in 2/15 (13%). The 1- and 3-year LC rates were 92% and 92%, respectively. The 1- and 3-year PFS rates were 79% and 32%, respectively, with a median PFS

of 24 months. The 1- and 3-year OS rates were 79% and 37%, respectively, with a median OS of 29 months (Figure 4).

Discussion

The development of ILNM tends to involve invasion of the skin and compression of nerves. Therefore, ILNM may cause pain and lymphedema in the lower extremities, which can impair patient's quality of life [1-3]. Surgery or EBRT are the primary treatment option for ILNM. Patients with ILNM often suffer from whole body metastasis and as such, they typically have lower KPS scores. For patients with advanced stage ILNM, surgery is not optimal, and EBRT is an alternative approach. Radiation fields will cover metastatic lesions and lymph draining

Table 1. Patients' clinical characteristics

Parameter	Value
Age (years), median (range)	61 (28-77)
Sex, n (%)	
Male	6 (40.0)
Female	9 (60.0)
Diagnosis, n (%)	
Rectal cancer	3 (20.0)
Cervical cancer	3 (20.0)
Endometrial carcinoma	2 (13.0)
Penile cancer	2 (13.0)
Ovarian cancer	1 (7.0)
Synovial sarcoma	1 (7.0)
Acinar soft tissue sarcoma	1 (7.0)
Neuro-endocrine carcinoma	1 (7.0)
Teratoma	1 (7.0)
Histologic type, n (%)	
Adenocarcinoma	6 (40.0)
Squamous cell carcinoma	5 (33.0)
Sarcoma	2 (13.0)
Neuro-endocrine carcinoma	1 (7.0)
Teratoma	1 (7.0)
Previous therapy, n (%)	
Surgery	11 (73.0)
Chemotherapy	7 (47.0)
Radiotherapy	11 (73.0)
Cumulative dose at implantation site EQD ₂ (Gy), median (range)	50 (0-80)
Symptom, n (%)	
Pain	12 (80.0)
Lower extremity edema	4 (27.0)
Karnofsky performance status at diagnosis, median (range)	80 (60-100)
Hemoglobin (g/l), median (range)	125 (86-152)
Pre-plan GTV (cm ³), median (range)	8.7 (0.8-185.1)

EQD₂ – equivalent dose in 2 Gy/fx., GTV – gross tumor volume

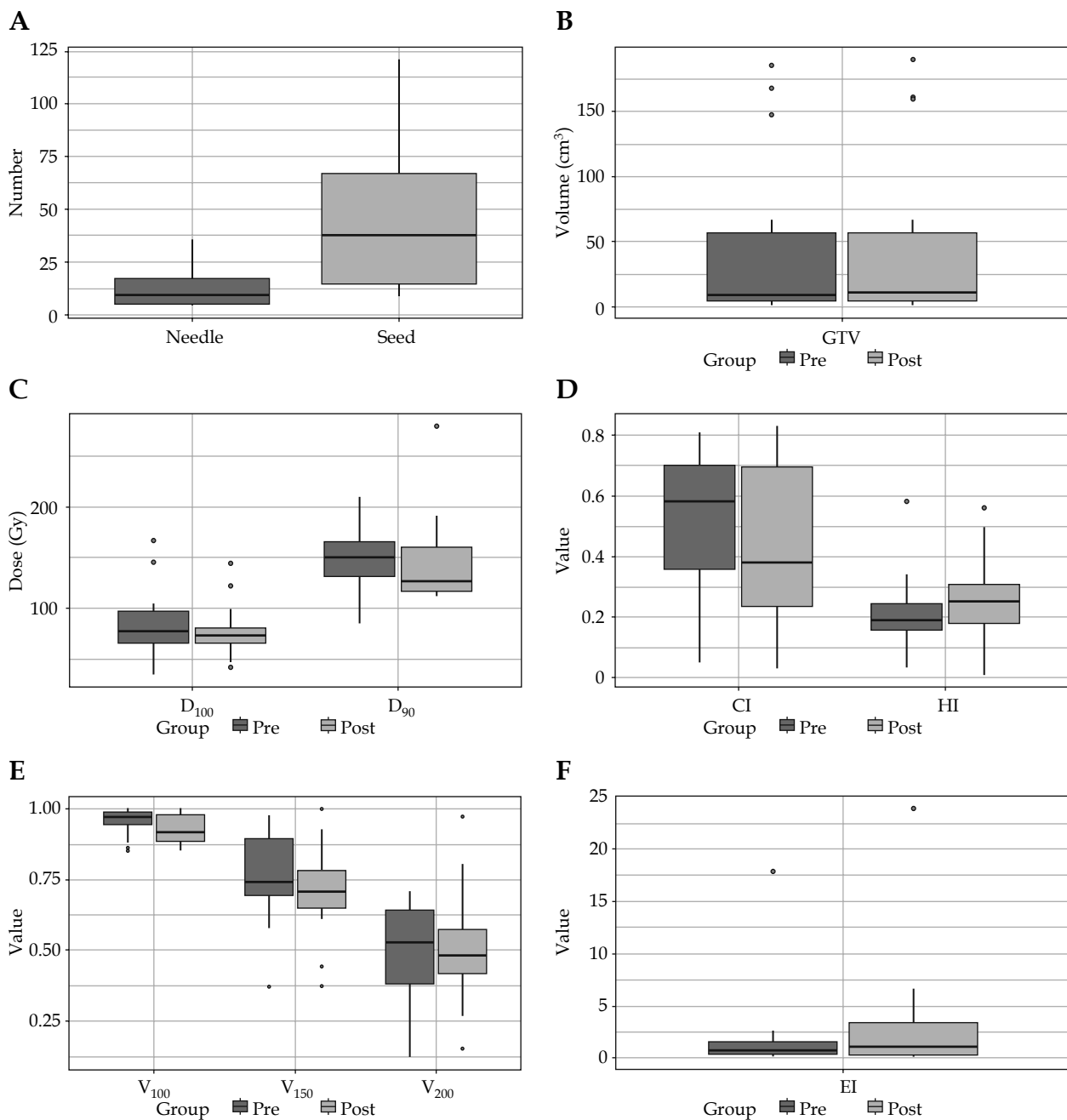


Fig. 2. Box-whisker plots of pre-plan and post-plan parameters. **A)** Numbers of needles and seeds. **B)** Volumes of pre-plan and post-plan gross tumor plots of pre-plan and post-plan parameters. **C)** Values of pre-plan and post-plan D_{90} and D_{100} . **D)** Values of pre-plan and post-plan conformal index (CI) and external index (EI). **E)** Values of pre-plan and post-plan V_{100} , V_{150} , and V_{200} . **F)** Values of pre-plan and post-plan EI. D_{90} - 90% absorbed dose of target volume; D_{100} - 100% absorbed dose of target volume; V_{100} , V_{150} , and V_{200} - percentage of 100%, 150%, and 200% prescribed dose coverage volume in target volume, respectively. HI - homogeneity index

regions, whilst the relatively long irradiated field and high doses may cause side effects, such as regional skin ulcers, fibrosis, and lymphedema [4-6, 18, 19].

With RISI, high doses can be delivered to the target, while surrounding normal tissues are spared with rapid dose drop-off, making the procedure an option for cancer treatment. Since RISI is a convenient procedure associated with minimal invasion, it allows patients to return to normal life within 1-2 days. However, the challenge of RISI lies in the accurate delivery of radioactive seeds into

the target. In 2002, CT-guided RISI offered a solution for delivering radioactive seeds into targets accurately [8-11], but it is still difficult to match post-plan dosimetric parameters with pre-plan requirements under a percutaneously CT-guided procedure, while OARs, such as blood vessels, bony anatomic structures, and nerves around the lesion may interfere with needle puncture. Furthermore, skills required for the puncture procedure vary among operators, which leads to great uncertainty and unrepeatability.

Table 2. Comparison of pre-operative and post-operative dosimetry parameters in target volume of 15 cases

Parameters	Pre-operative		Post-operative		p-value
	Region	$\bar{x} \pm s$	Region	$\bar{x} \pm s$	
D ₉₀ (Gy)	84.93-210.00	150.50 ±33.85	112.40-279.60	145.50 ±43.98	0.635
D ₁₀₀ (Gy)	34.58-166.90	84.33 ±35.94	41.78-144.80	77.98 ±26.69	0.479
V ₁₀₀	0.85-1.00	0.95 ±0.05	0.85-1.00	0.93 ±0.05	0.047
V ₁₅₀	0.37-0.97	0.76 ±0.17	0.37-1.00	0.70 ±0.16	0.044
V ₂₀₀	0.12-0.71	0.50 ±0.17	0.15-0.97	0.51 ±0.20	0.924
CI	0.05-0.81	0.52 ±0.22	0.03-0.83	0.43 ±0.26	0.009
EI	0.12-17.90	2.07 ±4.45	0.16-23.90	3.35 ±6.10	0.027
HI	0.03-0.58	0.21 ±0.13	0.01-0.56	0.25 ±0.14	0.068
GTV (cm ³)	0.80-185.10	45.57 ±65.57	1.70-189.50	46.47 ±66.78	0.614

Pre – pre-plan, Post – post-plan, CI – conformal index, EI – external index, HI – homogeneity index, D₉₀ – 90% absorbed dose of target volume, D₁₀₀ – 100% absorbed dose of target volume, V₁₀₀, V₁₅₀, and V₂₀₀ – percentage of 100%, 150%, and 200% of prescribed dose coverage volume in target volume, respectively

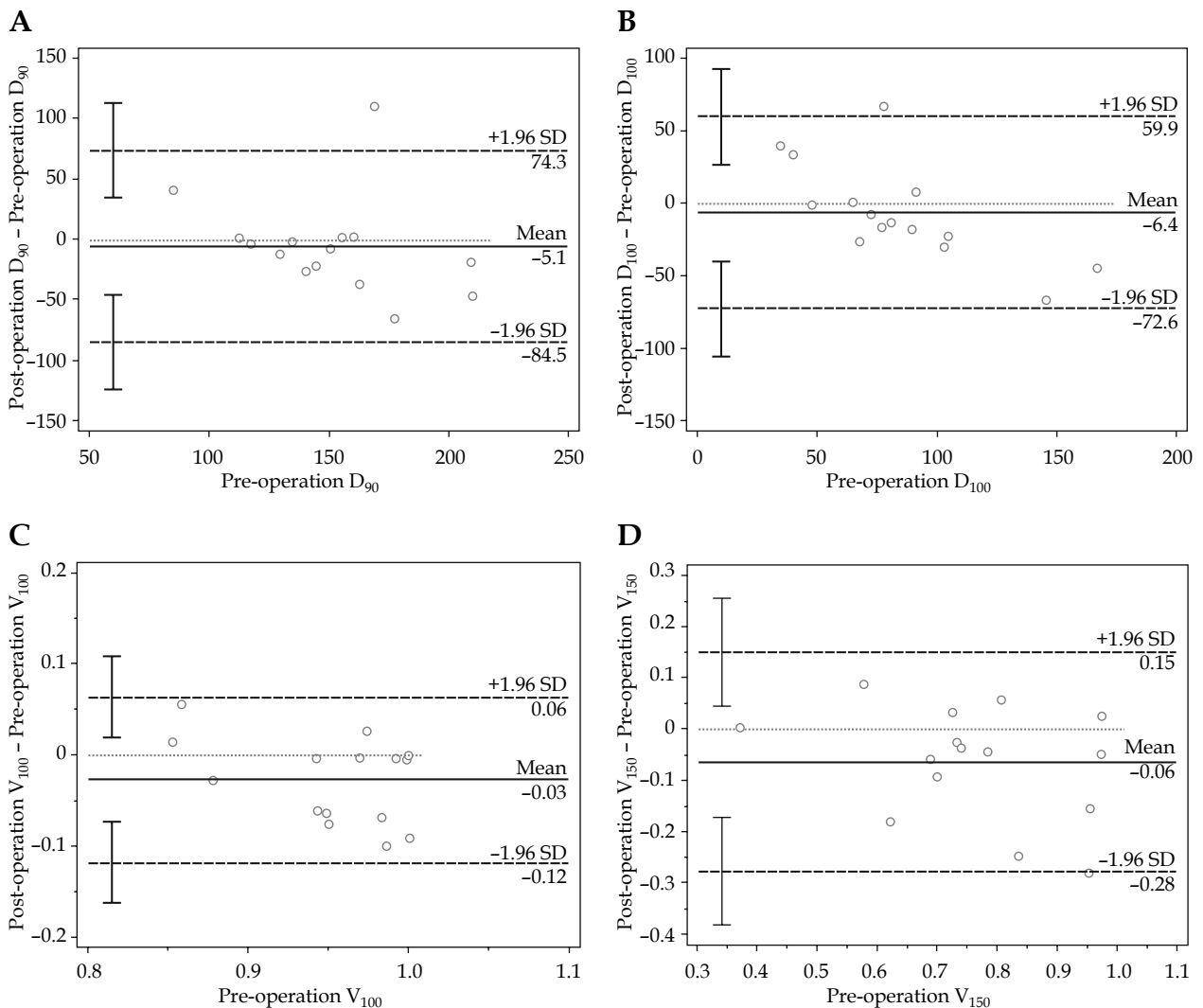


Fig. 3. Bland-Altman plot showing the difference between pre-plan and post-plan parameters with limits of agreement (LoA) (broken lines)

D₉₀ – 90% absorbed dose of target volume; D₁₀₀ – 100% absorbed dose of target volume; V₁₀₀, V₁₅₀, and V₂₀₀ – percentage of 100%, 150%, and 200% prescribed dose coverage volume in target volume, respectively; CI – conformal index; EI – external index; HI – homogeneity index; GTV – gross tumor volume

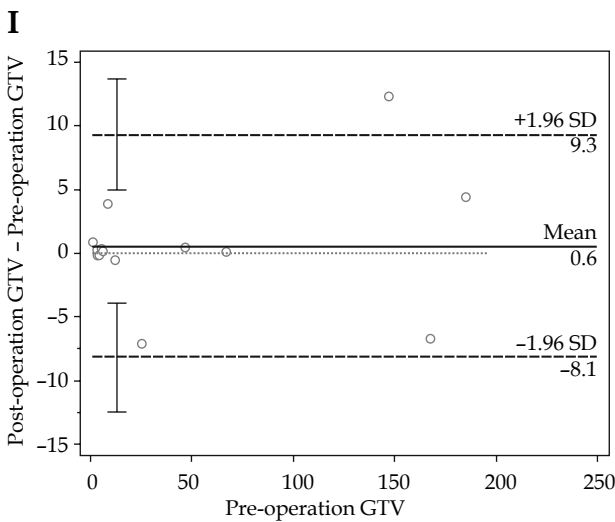
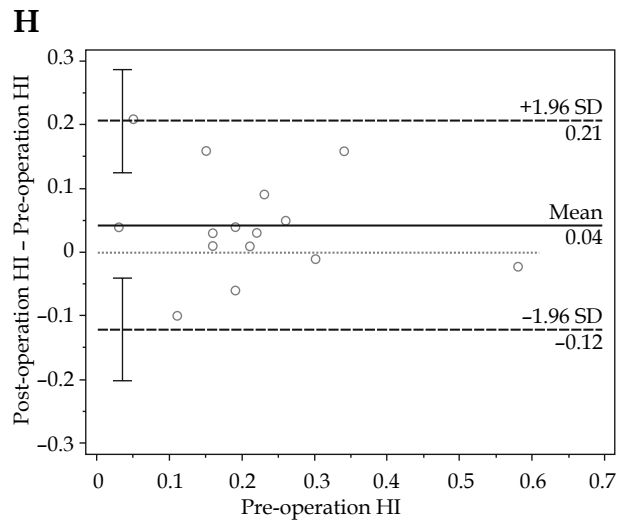
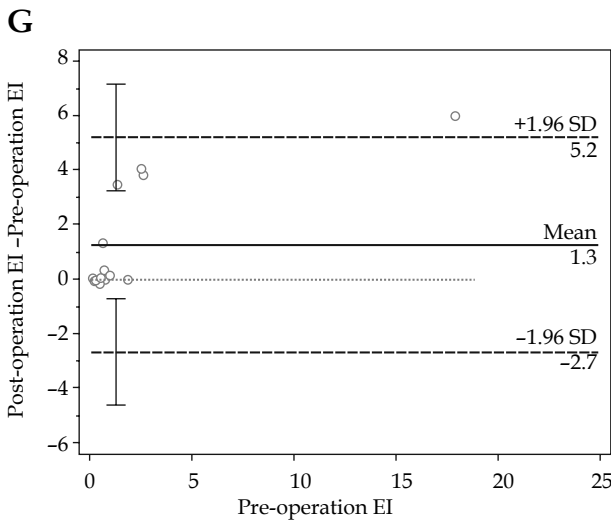
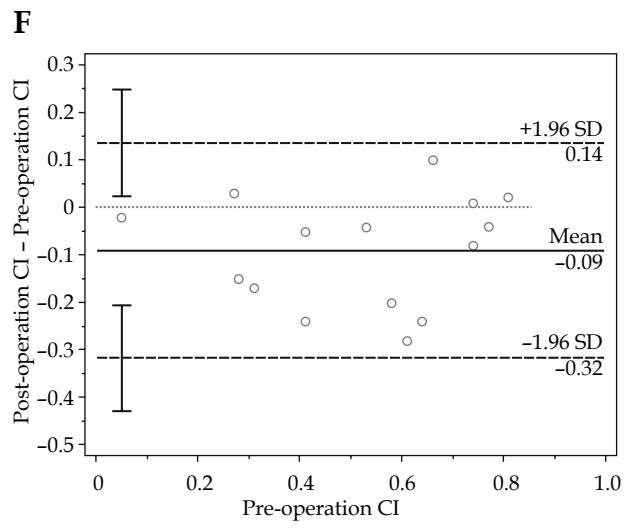
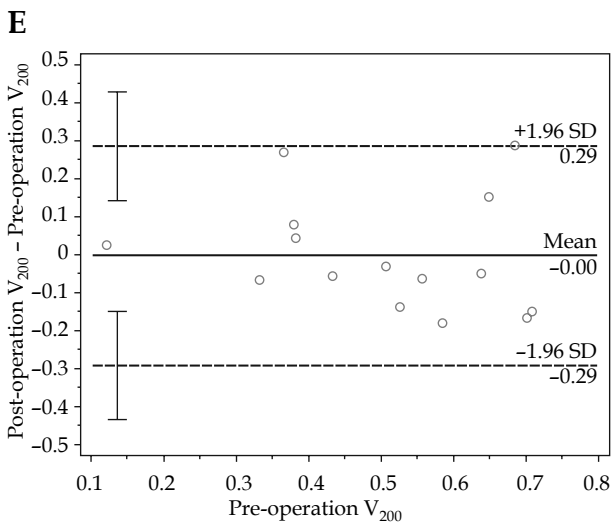


Fig. 3. Cont.

D_{90} – 90% absorbed dose of target volume; D_{100} – 100% absorbed dose of target volume; V_{100} , V_{150} , and V_{200} – percentage of 100%, 150%, and 200% prescribed dose coverage volume in target volume, respectively; CI – conformal index; EI – external index; HI – homogeneity index; GTV – gross tumor volume

3D-PNCT-assisted CT-guided RISI for body carcinomas was invented in 2015 [12-14]. Until then, 3D-PNCT has been applied to permanent interstitial BT for carcinomas in complex locations, such as the head and neck, the thorax, and the spinal cord as well as in recurrent pelvic cancers, pancreatic cancer, etc. [8-11, 20, 21]. The modality is safe and feasible, involving the positioning and accurate orientation of needle insertion through the alignment of external anatomic contours of patients. However, misalignment errors are of concern, especially for movable organs.

3D-PNCT-assisted CT-guided RISI is a procedure that is relatively easy to carry out and popularize. In addition, the cost of instruments and consumables involved are lower compared with EBRT. With the assistance of CT and 3D-PNCT, the physicians can accomplish RISI treatment independently after a three-month training program.

The inguinal region is suitable for the use of 3D-PNCT with the following advantages: 1) Lesion site is relatively superficial and stable, needle channels are short, and deviation is less likely to occur; 2) Bony anatomic structure facilitates easy 3D-PNCT fixation; and 3) Seed needles can be inserted from different directions. Therefore, not only can 3D-PNCT-assisted CT-guided RISI in the inguinal region meet target conformality while sparing OARs, but also it enables the procedure to be more accessible and easier to operate, with shorter treatment time.

Blood vessels are distributed in the inguinal region. The following methods have been adopted to avoid puncturing of blood vessels: 1) Acquiring images from either enhanced CT or MRI to make OARs margins clear; 2) Keeping the needles pathway in a safe distance of 0.5-1 cm from OARs, and reducing the activity of ^{125}I seeds to approximately 0.4 mCi; and 3) Keeping CTV with 2-3 mm margins from GTV when OARs are met. In our study, there were no blood vessel ruptures or bleeding when the above-mentioned safety measures were undertaken.

The location or volume of the targets might change after CT-simulation or during RISI. This could offset dosimetric parameters between the pre-plan and post-plan, even if the implantation was executed precisely. In view of this effect, the following measures to improve the dose distribution were taken: 1) The interval between CT-simulation and RISI was minimized, generally, no more than 2 days; 2) Before inserting the seed needles, 3 stable needles were innovatively inserted, which could fix both the template and tumor, to maximally reduce its' displacement caused by subsequent puncture; 3) If the tumor location or volume changed greatly, the intra-operative plan was adjusted, generally by adjusting the direction and depth of the needles, but occasionally, by increasing the number of needles or seeds. The additional needles could be inserted through holes reserved on the template. However, none of the 15 patients in the study had an increased number of needles or seeds.

Previous results of RISI for recurrent carcinomas have shown that prognosis was significantly affected by dosimetric parameters, such as D_{90} , D_{100} , and V_{100} . Achieving a post-plan D_{90} that is at least 90% of PD may result in the improvement of LC, OS, and PFS [9]. With 3D-PNCT and

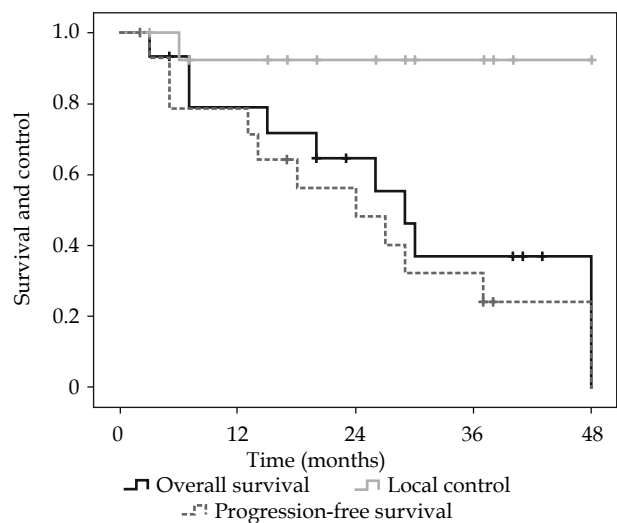


Fig. 4. Kaplan-Meier curves of local control, overall survival, and progression-free survival

CT guidance, the dosimetric parameters verified after RISI were able to meet the pre-plan requirements.

In this study, CT-guided 3D-PNCT greatly reduced misalignment errors and improved the accuracy of needles puncture. Under 3D-PNCT-assisted CT-guided procedure, each needle could be accurately placed in the target. Thus, the exact doses delivered to the targets could meet pre-plan requirements. A 3D-PNCT-assisted CT-guided procedure not only made the puncture procedure easy to performed, but also improved the accuracy of needles arrangement. 3D-PNCT combined with CT-guided RISI shortened the average operation by 30-60 minutes.

In this study, the BT-TPS was employing the American Association of Physicists in Medicine Task Group 43-recommended dosimetric parameters of sources, which are measured in water [22]. The effect of interseed attenuation for ^{125}I seeds, which may lead to dose calculation errors, was not considered. An analytical model to determine interseed attenuation effect was proposed in 2013 [23], and the development of new BT-TPS incorporating this model began a few years ago.

All 15 templates were accurately aligned and closely fitted to the skin marked lines with the stable needles. The mean post-operative D_{90} and D_{100} of the 15 lesions were 145.5 Gy and 78.0 Gy, respectively.

In our study, it was found that optimal pre-plan dosimetric parameters could be met in post-plan validation due to intra-operative real-time image guidance (case No. 6, case No. 10). However, if lesions (case No. 3 and case No. 7) were too large and adjacent to OARs, D_{90} and V_{100} could meet the requirement, while D_{100} was compromised to protect OARs.

CI and EI were important parameters for target conformality. In our study, the lesion volume varied greatly from 0.8 to 185.1 cm^3 . For large lesions, dose distribution could be easily optimized, but for small lesions, it was almost impossible to achieve both high doses in GTV and low doses out of GTV, since each seed would affect the area around itself, with a range of 1 cm. Therefore,

the CI and EI in the smaller lesions tended to be suboptimal. However, our study showed higher doses to GTV with less radiation to the surrounding normal tissues than those of patients with larger lesions.

The paired *t*-test showed that RISI could meet the requirements of pre-plan PD and limit hot-spot area. Paired *t*-test was used to compare the mean values of pre- and post-plan dosimetric parameters, which mainly indicated systematic errors. There were no significant statistical differences between the pre-plan and post-plan dosimetric parameters in D_{90} , D_{100} , V_{200} , HI, and GTV for ILNM treated with 3D-PNCT-assisted RISI. However, there were significant statistical differences in V_{100} , V_{150} , CI, and EI. As mentioned above, the indices of D_{90} , D_{100} , and V_{100} influenced the efficacy of RISI. The GTV of the post-plan was slightly larger than that of the pre-plan; however, the difference was not statistically significant. The contributing factors were as follows: 1) Tumor volume was increased from focal hematoma or edema associated with puncture; 2) The lesion boundary blurred due to puncture procedures, and even the enhanced CT images could not differentiate the lesion boundary, which might have caused target delineation errors.

Bland-Altman analysis indicated that the accidental error of RISI was small. The D_{90} and D_{100} in 1 of the 15 cases exceeded the pre-plan. Owing to the intra-operative real-time optimizations, the dose could be increased and delivered to the target area accurately. Among the 15 cases, there was only one case with V_{150} , EI, and GTV outside the specified accuracy range (95% CI), which may have been influenced by seed movement when the applicator was withdrawn. The V_{100} , V_{200} , CI, and HI of the 15 patients were within the specified accuracy range, which indicated that the accidental errors of these parameters were small. In the future, strand seeds will be able to resolve these differences.

RISI showed a favorable local control rate and pain relief. There were 9 cases (60%) with CR, and a 3-year LC rate of lesions was 92%. This was attributed to the improved therapeutic accuracy and high doses irradiated to targets. After RISI, 11 of 12 (92%) patients experienced pain reduction or complete remission, and no side effects greater than grade 1 were observed.

3D-PNCT-assisted CT-guided RISI could be an alternative option for patients with ILNM. The standard of care for patients with ILNM is surgery at the moment, and EBRT is also a primary choice. Currently, stereotactic body radiotherapy (SBRT) is one of the emerging radiation treatment techniques, in which ultra-fractionated dose can be delivered to the tumor, especially for small tumors, such as exclusive lymph node metastasis. Compared with SBRT, RISI only need one single implantation without too strict immobilization or breathing control, or gold fiducials implantation in some situations. To the best of our knowledge, there is limited evidence to compare the safety and efficacy of RISI and SBRT on treating lymph node metastasis (LNM), especially in ILNM. To date, it was reported that when treating exclusive LNM, LC was higher than 80% in nearly all cases regardless of the location, with PFS at 3 years higher than 20% and

2-year OS over 90% [24-27]. By contrast, LC and PFS rates in our studies were similar to those of SBRT series, while OS rates of 79% at 1 year were slightly lower in our study. Possible reasons were: 1) GTV was larger in our studies, compared to lesions of SBRT series usually less than 3 cm in diameter, which might indicate more invasive lesions in this study; 2) Lower OS rates might be associated with perioperative complications resulting from implantation; 3) The interval between primary treatment and RISI of most patients in our study was less than 12 months, which was an unfavorable prognostic factor in SBRT series.

Generally, our study showed that RISI proved to be minimally invasive, accessible, and time saving, and had a favorable therapeutic effect with lower toxicity. It is an effective salvage treatment for patients with prior EBRT in the inguinal region, for non-surgical candidates, and patients with limited mobility, or patients refused surgery. It is also suitable for patients with an advanced age or as a palliative therapy. Our study was limited by a small sample size of 15 patients, and a larger cohort study is warranted in the future.

Conclusions

3D-PNCT-assisted CT-guided RISI is a feasible, safe, and accurate treatment modality for ILNM. The pre-plan can be accurately executed by 3D-PNCT-assisted CT-guided RISI.

Funding

The study was supported by a grant from the Peking University (grant No.: BMU2017JC001-3).

Disclosure

The authors report no conflict of interest.

References

1. National Comprehensive Cancer Network. Cervical Cancer (Version 1.2022). Available from: https://www.nccn.org/professionals/physician_gls/pdf/cervical.pdf.
2. National Comprehensive Cancer Network. Rectal Cancer (Version 1.2022). Available from: https://www.nccn.org/professionals/physician_gls/pdf/rectal.pdf.
3. National Comprehensive Cancer Network. Penile Cancer (Version 2.2022). Available from: https://www.nccn.org/professionals/physician_gls/pdf/penile.pdf.
4. Ballo MT, Zagars GK, Gershenwald JE et al. A critical assessment of adjuvant radiotherapy for inguinal lymph node metastases from melanoma. *Ann Surg Oncol* 2004; 11: 1079-1084.
5. Pagliaro LC, Crook J. Multimodality therapy in penile cancer: when and which treatments? *World J Urol* 2009; 27: 221-225.
6. Heyns CF, Fleshner N, Sangar V et al. Management of the lymph nodes in penile cancer. *Urology* 2010; 76 (2 Suppl 1): S43-57.
7. Hinnen KA, Battermann JJ, van Roermund JGH et al. Long-term biochemical and survival outcome of 921 patients treated with I-125 permanent prostate brachytherapy. *Int J Radiat Oncol Biol Phys* 2010; 76: 1433-1438.
8. Ji Z, Jiang Y, Tian S et al. The effectiveness and prognostic factors of CT-guided radioactive I-125 seed implantation for the treatment of recurrent head and neck cancer after exter-

- nal beam radiation therapy. *Int J Radiat Oncol Biol Phys* 2019; 103: 638-645.
9. Qu A, Jiang P, Sun H et al. Efficacy and dosimetry analysis of image-guided radioactive (125)I seed implantation as salvage treatment for pelvic recurrent cervical cancer after external beam radiotherapy. *J Gynecol Oncol* 2019; 30: e9.
 10. Jiang YL, Meng N, Wang JJ et al. Percutaneous computed tomography/ultrasonography-guided permanent iodine-125 implantation as salvage therapy for recurrent squamous cell cancers of head and neck. *Cancer Biol Ther* 2010; 9: 959-966.
 11. Liu Y, Jiang P, Zhang H et al. Safety and efficacy of 3D-printed templates assisted CT-guided radioactive iodine-125 seed implantation for the treatment of recurrent cervical carcinoma after external beam radiotherapy. *J Gynecol Oncol* 2021; 32: e15.
 12. Ji Z, Jiang Y, Guo F et al. Dosimetry verification of radioactive seed implantation for malignant tumors assisted by 3D printing individual templates and CT guidance. *Appl Radiat Isot* 2017; 124: 68-74.
 13. Ji Z, Jiang Y, Su L et al. Dosimetry verification of (125)I seeds implantation with three-dimensional printing noncoplanar templates and CT guidance for paravertebral/retroperitoneal malignant tumors. *Technol Cancer Res Treat* 2017; 16: 1044-1050.
 14. Wang J, Zhang F, Guo J et al. Expert consensus workshop report: Guideline for three-dimensional printing template-assisted computed tomography-guided (125)I seeds interstitial implantation brachytherapy. *J Cancer Res Ther* 2017; 13: 607-612.
 15. International Commission on Radiological Protection. Radiation safety aspects of brachytherapy for prostate cancer using permanently implanted sources. A report of ICRP Publication 98. *Ann ICRP* 2005; 35: iii-vi, 3-50.
 16. Gurram L, Wadasadawala T, Joshi K. Multi-catheter interstitial brachytherapy for partial breast irradiation: an audit of implant quality based on dosimetric evaluation comparing intra-operative versus post-operative placement. *J Contemp Brachytherapy* 2016; 8: 116-121.
 17. Cox JD, Stetz J, Pajak TF. Toxicity criteria of the Radiation Therapy Oncology Group (RTOG) and the European Organization for Research and Treatment of Cancer (EORTC). *Int J Radiat Oncol Biol Phys* 1995; 31: 1341-1346.
 18. Stecklein SR, Frumovitz M, Klopp AH et al. Effectiveness of definitive radiotherapy for squamous cell carcinoma of the vulva with gross inguinal lymphadenopathy. *Gynecol Oncol* 2018; 148: 474-479.
 19. Leone A, Diorio GJ, Pettaway C et al. Contemporary management of patients with penile cancer and lymph node metastasis. *Nat Rev Urol* 2017; 14: 335-347.
 20. Jiang Y, Ji Z, Guo F et al. Side effects of CT-guided implantation of (125)I seeds for recurrent malignant tumors of the head and neck assisted by 3D printing non co-planar template. *Radiat Oncol* 2018; 13: 18.
 21. Ji Z, Jiang Y, Guo F et al. Safety and efficacy of CT-guided radioactive iodine-125 seed implantation assisted by a 3D printing template for the treatment of thoracic malignancies. *J Cancer Res Clin Oncol* 2020; 146: 229-236.
 22. Nath R, Anderson LL, Luxton G et al. Dosimetry of interstitial brachytherapy sources: recommendations of the AAPM Radiation Therapy Committee Task Group No. 43. American Association of Physicists in Medicine. *Med Phys* 1995; 22: 209-234.
 23. Safigholi H, Sardari D, Jashni SK et al. An analytical model to determine interseed attenuation effect in low-dose-rate brachytherapy. *J Appl Clin Med Phys* 2013; 14: 4226.
 24. Battaglia A, De Meerleer G, Tosco L et al. Novel insights into the management of oligometastatic prostate cancer: a comprehensive review. *Eur Urol Oncol* 2019; 2: 174-188.
 25. Conde-Moreno AJ, Lopez-Guerra JL, Macias VA et al. Spanish Society of Radiation Oncology clinical guidelines for stereotactic body radiation therapy in lymph node oligometastases. *Clin Transl Oncol* 2016; 18: 342-351.
 26. Chen H, Louie AV, Higginson DS et al. Stereotactic radiosurgery and stereotactic body radiotherapy in the management of oligometastatic disease. *Clin Oncol (R Coll Radiol)* 2020; 32: 713-727.
 27. Hong JC, Salama JK. The expanding role of stereotactic body radiation therapy in oligometastatic solid tumors: What do we know and where are we going? *Cancer Treat Rev* 2017; 52: 22-32.